

RSC Advances



This is an *Accepted Manuscript*, which has been through the Royal Society of Chemistry peer review process and has been accepted for publication.

Accepted Manuscripts are published online shortly after acceptance, before technical editing, formatting and proof reading. Using this free service, authors can make their results available to the community, in citable form, before we publish the edited article. This *Accepted Manuscript* will be replaced by the edited, formatted and paginated article as soon as this is available.

You can find more information about *Accepted Manuscripts* in the [Information for Authors](#).

Please note that technical editing may introduce minor changes to the text and/or graphics, which may alter content. The journal's standard [Terms & Conditions](#) and the [Ethical guidelines](#) still apply. In no event shall the Royal Society of Chemistry be held responsible for any errors or omissions in this *Accepted Manuscript* or any consequences arising from the use of any information it contains.

Novel ^{99m}Tc radiolabeled folate complexes with PEG linkers for FR-positive tumor imaging: synthesis and biological evaluation

Fang Xie^a, Chun Zhang^b, Qian Yu^a, Yan Pang^a, Yuan Chen^a, Wenjiang Yang^c, Jingquan Xue^c, Yu Liu^c, Jie Lu^{a,*}

^a Key Laboratory of Radiopharmaceuticals (Beijing Normal University), Ministry of Education; College of Chemistry, Beijing Normal University, Beijing 100875, P. R. China

^b Department of Nuclear Medicine, Beijing Chao-Yang Hospital, Capital Medical University, Beijing 100020, P. R. China

^c Key laboratory of Nuclear Radiation and Nuclear Energy Technology, Institute of High Energy Physics, China Academy of Sciences, Beijing 100142, P. R. China

* Corresponding author (Jie Lu): E-mail: ljie74@bnu.edu.cn; Tel: +86 010 62208126; Fax: +86 010 62208126. Fang Xie and Chun Zhang contributed equally to this work.

Abstract

In order to develop a novel ^{99m}Tc -labeled folate based SPECT radiotracer with optimized pharmacokinetic profile for the folate receptor (FR) positive tumors imaging, a folate conjugate, HYNIC-PEG2-FA, was designed, synthesized and radiolabeled with ^{99m}Tc using tricine/ diphenylphosphinobenzene-3-sulfonic acid sodium (TPPMS), tricine/trisodium triphenylphosphine-3,3',3''-trisulfonate (TPPTS), and ethylenediamine-N,N'-diacetic acid (EDDA) as coligands. $^{99m}\text{Tc}(\text{HYNIC-PEG2-FA})(\text{tricine}/\text{TPPTS})$, **4**, $^{99m}\text{Tc}(\text{HYNIC-PEG2-FA})(\text{tricine}/\text{TPPMS})$, **5** and $^{99m}\text{Tc}(\text{HYNIC-PEG2-FA})(\text{EDDA})$, **6**, were obtained respectively. All of them were stable in saline and mice plasma for 6 h, and displayed high specific binding in FR-positive KB cell line *in vitro*. Among them, complex **4** exhibited a higher tumor uptake ($11.35 \pm 0.67\% \text{ID/g}$ at 2 h p.i.) and more rapid clearance from liver, lungs, blood, muscle and other non-target organs than $^{99m}\text{Tc}(\text{HYNIC-NHHN-FA})(\text{tricine}/\text{TPPTS})$, which we reported before. Small animal SPECT/CT imaging studies in FR-positive KB tumor models showed that the tumor could be clearly visualized at 120 min p.i., suggesting its potential as a promising folate receptor targeted agent for tumor imaging.

Keywords: Technetium-99m; Folate receptor; Folate derivative; Tumor targeting, Tumor imaging

1. Introduction

The folate receptor (FR), a glycosylphosphatidylinositol-anchored membrane glycoprotein, is over-expressed in approximated 100% of ovarian adenocarcinomas and various epithelial cancers, such as breast, colorectal, renal and cervical cancers.¹⁻³ The FR binds the vitamin folic acid with high affinity ($K_d \approx 10^{-10}$ M), and mediates the transport of folic acid into cell interior via an endocytic process.⁴ Thus, the folate receptor has been respected as a very attractive molecular target for the development of tumor selective therapeutic drugs and molecular imaging agents.⁵⁻⁸ Many radiolabeled folate-conjugates have been developed for single photon emission computed tomography (SPECT) and positron emission tomography (PET) imaging.⁸⁻¹¹ Among them, ¹¹¹In-DTPA-folate¹²⁻¹⁴ and ^{99m}Tc-EC20^{15,16} have been tested in clinical trials. These highlight the potential of folate-based radiotracers as noninvasive diagnostic tools to visualize the FR-positive tumor.

For SPECT imaging, ^{99m}Tc is the most attractive radionuclide due to its favorable nuclear properties ($E_\gamma = 140$ KeV, $T_{1/2} = 6.02$ h), easy availability and low cost. Gou *et al.*¹⁷ reported the synthesis and evaluation of a ^{99m}Tc-labeled folate-hydrazide-HYNIC conjugate. 6-hydrazinonicotinic acid (HYNIC) served as the bifunctional coupling agent due to its high labeling efficiency at low HYNIC-conjugate concentrations. The ^{99m}Tc-HYNIC-folate displayed considerable and FR-specific tumor uptakes in biodistribution studies. Recently, we have reported a novel class of ^{99m}Tc- labeled FA-NHHN-HYNIC conjugates for the folate receptor imaging (Fig. 1).¹⁸ A hydrocarbon linker was introduced between the HYNIC and folate to increase the distance between target moiety and chelating group. Compare to the short hydrazide linker of the ^{99m}Tc-HYNIC-folate, the longer hexane linker of the ^{99m}Tc(HYNIC-NHHN-FA)(tricine/TPPTS) exhibited more favorable tumor targeting properties.^{18,19}

It is highly desirable to develop novel folate-based radiotracer with optimistic excretion kinetics, so that a high target-to-background (T/B) ratio can be obtained for FR-positive tumor imaging in a short period of time. In this study, we designed and synthesized a novel folate conjugate with a more hydrophilic and longer linker, HYNIC-PEG2-FA (Fig. 1). The small polyethylene glycol (PEG2) linker

was used for two purposes: (1) to increase the distance between the folic moiety and the ^{99m}Tc -HYNIC chelating group, (2) to improve the tumor uptake and excretion kinetics from non-targeting organs. Since many previous studies have shown that the coligand has played an important role on the biological properties of ^{99m}Tc -HYNIC complexes,²⁰⁻²³ herein we labeled HYNIC-PEG2-FA using three different coligands: tricine/TPPTS, tricine/TPPMS and EDDA (Fig. 1). *In vitro* and *in vivo* evaluations of these complexes have been done to investigate their biological properties and the impact of the coligands on the affinity and pharmacokinetic profile.

2. Experiment section

2.1 Materials

2,2'-(ethylenedioxy)-bis-ethylamine, 4-Dimethylaminobenzaldehyde, Di-tert-butyldicarbonate, Trifluoroacetic acid, Dicyclohexylcarbo-diimide were purchased from Alfa Aesar China (Tianjin) Co., Ltd. *N*-tris-(hydroxymethyl)-methylglycine (Tricine), trisodium triphenylphosphine-3,3',3''- trisulfonate (TPPTS), diphenylphosphinobenzene-3-sulfonic acid sodium (TPPMS) and ethylenediamine-*N,N'*-diacetic acid (EDDA) were purchased from ACROS Organics USA. All other chemicals were of reagent grade. Technetium-99m as sodium pertechnetate ($\text{Na}^{99m}\text{TcO}_4$) was obtained from commercial $^{99}\text{Mo}/^{99m}\text{Tc}$ generator (China Institute of Atom Energy). NMR spectra were recorded on Bruker Avance III (400 MHz) spectrometers. LC-MS (ESI-MS) was performed on ACQUITY UPLC system (Waters, Milford, MA, USA), and Micromass Quattro micro API mass spectrometer (Waters, Milford, MA) and HRMS was recorded on a Bruker micro TOF-QII mass spectrometer. Reversed-phase high pressure liquid chromatography (RP-HPLC) experiments were performed on a SHIMAZU LC-20AT HPLC pump system (SHIMAZU Corporation, Japan) equipped with a UV/vis detector ($\lambda = 254 \text{ nm}$) and a BIOSCAN flow-counter, using Venusil XBP C18 column(250×10mm, 5- μm particle size, Agela Technologies, USA). The gradient mobile phase were, Method 1, A: 0.05% $\text{NH}_3 \cdot \text{H}_2\text{O}$ (V/V), B: 100% CH_3OH ; 0~10min, 95~50% B, 10~20min, 50% B, 20~30min, 50~5% B; flow rate: 1 mL/min. Method 2, A: 90% NH_4HCO_3 (0.05 mol/L pH 7.0) /10% CH_3OH , B: 100% CH_3OH ; 0~10min, 95~50% B, 10~20min, 50% B, 20~30, 50~5%

B; flow rate: 1 mL/min. Imaging studies were performed on a small animal SPECT/CT scanner (Eplus-166, Institute of High Energy Physics, Chinese Academy of Sciences).

2.2 Synthetic procedures

The synthesis of the conjugate HYNIC-PEG2-FA is shown in Fig. 2. A small PEG, 2, 2'-(ethyleneoxy)-bis-ethylamine was used as a linker between folic acid and HYNIC to increase the range of accessible receptor sites and the water solubility of the conjugate. Reaction of PEG2-FA, **2** with N-hydroxysuccinimide activated hydrazononicotinate (NHS-HYNIC) gave conjugate **3** in good yield and in high purity (> 95%) after HPLC purification. Its chemical structure was characterized by ^1H NMR, ^{13}C NMR, ESI-MS and HRMS.

The Boc-monoprotected PEG2, tert-Butyl-{2-[2-(2-aminoethoxy)ethoxy]ethyl}-carbamate and succinimidyl 6-[2-(4-Dimethylamino) benzaldehydehydrazono] nicotinate (NHS-HYNIC) were synthesized according to the literatures.^{24,25}

2.2.1 Synthesis of compound Boc-PEG2-FA, **1**:

In the dark under a nitrogen atmosphere at room temperature, to a solution of folic acid (902 mg, 2.04 mmol) in anhydrous dimethyl sulfoxide (DMSO, 60 mL) and pyridine (30 mL) were added the tert-Butyl-{2-[2-(2-aminoethoxy)ethoxy]ethyl}-carbamate (620 mg, 2.50 mmol) and dicyclohexylcarbodiimide (DCC) (1.54 g, 7.50 mmol). After been stirred at room temperature for 18 h, the reaction mixture was filtered and gradually poured into a vigorously stirred solution of Et₂O (ice cold). The yellow precipitate was collected by filtration, washed with Et₂O (2×50 mL) and dried under high vacuum to afford 985 mg of compound **1**, yield 89.1%. This material was used for the next step without further purification. ^1H NMR (400 MHz, DMSO-*d*₆) δ : 8.63 (s, 1H), 7.90-7.84 (m, 2H), 7.66 (d, 2H, $J = 8.8\text{Hz}$), 6.95 (m, 2H), 6.73 (s, 1H), 6.65 (d, 2H, $J = 8.8\text{ Hz}$), 4.49 (s, 2H), 4.37-4.33 (m, 1H), 3.75-3.40 (overlap, 8H), 3.25-3.19 (m, 2H), 3.05 (m, 2H), 2.26-1.82 (m, 4H), 1.36 (s, 9H).

2.2.2 Synthesis of compound PEG2-FA, **2**:

Under a nitrogen atmosphere at 0 °C, compound **1** (760 mg, 1.13mmol) was treated with trifluoroacetic acid (TFA) (1 ml). After being stirred for 2 h, TFA was evaporated under high vacuum. The residue was

washed with Et₂O (2×50 ml) to get compound PEG2-FA (580mg, 1.02mmol), yield 90.3%. This material was used for the next step without further purification. ¹H NMR (400 MHz, DMSO-*d*₆) δ: 8.65 (s, 1H), 8.13-7.91 (m, 2H), 7.66 (d, 2H, *J* = 9.6Hz), 7.00 (m, 3H), 6.65 (d, 2H, *J* = 8.4Hz), 4.49 (s, 2H), 4.37-4.33 (m, 1H), 3.63-3.42 (overlap, 8H), 3.21 (m, 2H), 3.05 (m, 2H), 2.23-1.66 (m, 4H).

2.2.3 Synthesis of compound HYNIC-PEG2-FA, 3:

In the dark, succinimidyl 6-[2-(4-Dimethylamino) benzaldehydehydrazono] nicotinate (310 mg, 0.81 mmol) was added to a solution of compound **2** (280mg, 0.49mmol) in DMSO (15 mL) and pyridine (10 ml). After being stirred at room temperature for 18 h, the mixture solution was added dropwise into anhydrous Et₂O (50 ml). The red-yellow precipitate was collected by centrifugation, then washed with Et₂O and dichloromethane, dried under high vacuum to afford compound **3** (209mg, 0.25mmol), yield 51.0%. The product was purified by HPLC (method 1). The fraction at 24.1-25.5 min was collected. ¹H NMR (400 MHz, DMSO-*d*₆) δ: 8.95 (m, 1H), 8.61 (m, 2H), 7.97-7.84 (m, 2H), 7.66 (d, 4H, *J* = 8.5Hz), 7.36 (m, 2H), 6.92 (m, 1H), 6.61 (d, 3H, *J* = 8.0Hz), 5.42 (s, 2H), 4.45 (m, 2H), 4.34-4.32 (m, 1H,), 3.67-3.50 (overlap, 8H), 3.21-3.19 (m, 2H), 3.17 (s, 6H), 3.00-2.96 (m, 2H), 2.20-1.89 (m, 4H); ¹³C NMR (400 MHz, DMSO-*d*₆) δ: 210.7, 174.1, 171.8, 166.2, 165.0, 161.5, 161.1, 156.2, 155.7, 153.8, 150.7, 148.5, 147.8, 136.5, 129.0, 128.9, 127.9, 121.4, 120.4, 111.1, 104.5, 79.1, 69.5, 69.0, 66.6, 45.9, 41.3, 30.5, 28.0, 27.0, 26.4, 24.2; ESI-MS: *m/z* [M+H]⁺ calculated for C₄₀H₄₇N₁₃O₈: 838.4, found 838.7; HRMS [M+H]⁺ calculated for C₄₀H₄₇N₁₃O₈: 838.3743, found 838.3719.

2.3 Radiolabeling

The conjugate **3** was labeled with ^{99m}Tc using tricine/TPPTS, tricine/TPPMS, EDDA as coligands by a two-steps method.

In the first step, the labeling precursor, ^{99m}Tc (HYNIC-PEG2-FA)(tricine), was radiolabelled according to our published procedure.^{18,26} Briefly, FA-PEG2-HYNIC solution (50 μL, 1 mg/mL), acetate buffer solution (0.5 mL, pH = 3.6), tricine solution (0.5 mL, 80 mg/mL), SnCl₂ solution (20 μL, 2 mg/mL) in 0.1 N HCl and ^{99m}TcO₄⁻ in saline (0.2 mL, 37 MBq) was added into a 10 mL vial. The reaction mixture was heated at 100 °C for 15 min. After cooling to room temperature, the resulting solution was analyzed by

radio-HPLC.

Then, in the second step, 5 mg of co-ligand (TPPTS, TPPMS or EDDA) was added to the ^{99m}Tc (HYNIC-PEG2-FA)(tricine) labeling precursor solution described above. The mixture was heated at 100 °C for 15 min, then cooled to room temperature. The resulting solution was analyzed and purified by radio-HPLC (method 2) to obtain ^{99m}Tc (HYNIC-PEG2-FA)(tricine/TPPTS), **4**, ^{99m}Tc (HYNIC-PEG2-FA)(tricine/TPPMS), **5** and ^{99m}Tc (HYNIC-PEG2-FA)(EDDA), **6** respectively, for next experiments.

2.4 Stability study

The purified ^{99m}Tc -labeled radiotracers solutions were dissolved in saline and kept at room temperature, after 6 h, the resulting solutions were analyzed by radio-HPLC for the stability study in saline.

For the stability study in plasma, 100 μL of the purified radiotracers solutions were added to 900 μL of fresh mouse plasma and incubated at 37°C. After incubation for 6 h, the solutions were treated with 1 mL of ethanol to precipitate the proteins, after centrifuging at 3000 rpm. The supernatants were analyzed by radio-HPLC.

2.5 Determination of the octanol/water partition coefficient ($\log P$)

To determine the octanol/water partition coefficient, a sample of 0.1 mL of the purified radiotracer solution was mixed with 0.6 mL of phosphate buffer (0.05mol/L, pH = 7.4) and 0.7 mL of octanol in a centrifuge tube. The mixture was vortexed for 3 min and centrifuged at 4000 rpm for 5 min. 0.1 mL aliquots of octanol and phosphate buffer were counted by NaI well-type γ -counter. Based on the definition of the octanol/water partition coefficient ($\log P$), $P = (\text{concentration of tracer in octanol})/(\text{concentration of tracer in aqueous layer})$, the value of P was determined by: $P = (\text{activity in octanol-background activity})/(\text{activity in aqueous layer-background activity})$.¹⁸ All experiments were performed in triplicate.

2.6 *In vitro* cell studies

Cell binding experiments were performed in KB carcinoma cell line and mouse normal fibroblast NIH/3T3 cell line by the previous method.^{18,26,27} The KB and NIH/3T3 cells were cultured as monolayer at 37 °C in a humidified atmosphere containing 5% CO_2 . The cells were cultured in a folic acid free medium, FFRPMI medium (modified RPMI 1640 medium without folic acid), supplemented with 10%

fetal calf serum (FCS), and antibiotics (penicillin 100 IU/ml, streptomycin 100 µg/ml, fungizone 0.25 µg/ml).

The KB and NIH/3T3 cells were seeded in 24-well plates (2×10^5 cells/well) 24 hours prior to the experiment to form confluent monolayer at 37 °C. After being washed once with FFRPMI medium, the cells were incubated at 37 °C for 1 h with approximately 7.4 KBq of HPLC purified radiotracer in 1 ml of FFRPMI medium. The blocking studies were performed by addition of free folic acid solution (10 µl, 1 mg/ml) into the incubation medium. After incubation, the reaction media were aspirated, and the cells were rinsed with 2×1 ml of cold PBS (pH 7.4). Washing the cells with 1 ml of acidic buffer (aqueous solution of 0.1 M acetic acid and 0.15 M NaCl, pH = 3) to assess cellular internalization of the ^{99m}Tc radiotracer. Finally, the cells were lysed by treatment with 1 ml of 1 N NaOH for 5 min. The samples were counted by γ -counter. Cellular protein was determined by using BCA protein assay reagent. The cell binding fractions and cell internalized fractions were calculated per 0.5 mg protein and expressed in relation to the total added activity (% per 0.5 mg protein of total added activity). All experiments were performed in triplicate.

2.7 Biodistribution Studies

All experiments concerned about animals were carried out in compliance with the national laws related to the conduct of animal experimentation.

2.7.1 Biodistribution Studies in normal mice

The biodistribution studies were performed in normal Kunming mice. Before the experiments, the normal Kunming mice (18-20g weight) were fed with a folate-free diet for 7 days. Then 0.1 mL of the HPLC-purified radiotracer solution (~ 111 kBq) was injected into the mice via the tail vein. The mice (n = 5) were sacrificed by cervical dislocation at 60, 120 and 240 min after injection. For blocking studies, excess folic acid (100 µg/mouse) was co-injected prior to the radiotracer injection, and the mice were sacrificed at 60 min postinjection. The Selected tissues and organs were removed, weighed and measured in a well-type NaI (TI) γ -counter. The percentage of injected dose per gram (%ID/g) for each sample was

calculated by comparing its activity with appropriate standard of injected dose (ID). The values were expressed as mean \pm SD.

2.7.2 Biodistribution Studies in KB tumor-bearing mice

The athymic BALB/c mice were injected 5×10^6 cells of FR- positive KB cells to establish the KB tumor model mice. After inoculation of 14~16 days and feeding with a folate-free diet, the mice with 0.5~1.0 cm³ tumor were used for biodistribution studies. 0.1 mL of the HPLC-purified radiotracer solution (\sim 111 kBq) was injected into the KB tumor bearing mice via the tail vein, the mice (n = 3) were sacrificed by cervical dislocation at 120 min post-injection. Co-injection of excess folic acid (100 μ g/mouse) was performed for blocking studies. The selected tissues and organs were removed, weighed and measured in a well-type NaI (TI) γ -counter. The percentage of injected dose per gram (%ID/g) for each sample was calculated by comparing its activity with appropriate standard of injected dose (ID). The values were expressed as mean \pm SD.

2.8 Small animal SPECT/CT imaging studies

Imaging studies of ^{99m}Tc (HYNIC-PEG2-FA)(tricine/TPPTS), **4** were performed in the athymic nude mice bearing KB tumors. The purified radiotracers (\sim 14.8 MBq) in saline were injected via the tail vein. The mice were anesthetized with 1.5% isoflurane for imaging at 120 min post-injection. The data was acquired using a small animal SPECT/CT scanner, which consists of a NaI(Tl)-based detector equipped with a parallel hole collimator having a FOV of 80mm \times 80mm, an average energy resolution of 11.5% and a sensitivity of 38cps/MBq with a \pm 10% energy window. The emission projection data were acquired in list mode format and Fourier rebinned into two-dimensional (2D) sinograms. Images were then reconstructed using the 2D OSEM algorithm (5 iterations and 6 subsets), resulting in 0.5 \times 0.5 \times 1.6 mm³ voxel size for a 256 \times 256 \times 50 image volume. The CT subsystem includes a standard self-contained, air-cooled x-ray tube operating at a maximum tube voltage of 90 kV and a maximum tube current of 200 μ A. The CT images were reconstructed using 3D cone-beam Feldkamp algorithm into 0.25 \times 0.25 \times 0.25mm³ voxel size in a 512 \times 512 \times 512 image matrix. After cropped to SPECT

image size, down-sampled to SPECT voxel size, the registered CT images were then reconstructed with an affine transform and linear interpolation.

2.9 Statistical analysis

Statistical analysis was performed using the Student's t-test for unpaired data to determine the significance of differences between the groups in the studies of specificity of cellular uptake and biodistribution described above. Difference at the 95% confidence level ($p < 0.05$) was considered significant.

3. Results

3.1 Radiochemistry

The complex **4**, **5** and **6** were successfully prepared by using ^{99m}Tc (HYNIC-PEG2-FA)(tricine) as labeling precursor. Fig. 3 shows the HPLC chromatograms of the four complexes. The precursor, ^{99m}Tc (HYNIC-PEG2-FA) (tricine), was prepared in yield more than 90%, and the retention time is 15.4 min. When the co-ligands added, successful ligand exchanges were evidenced by disappearance of the peak at 15.4 min and formation of new peaks. The HPLC retention times of complex **4**, **5** and **6** were 22.5, 28.3 and 21.4 min, respectively. The radiotracers were completely separated from its excess unlabeled folate conjugates by HPLC. The radiochemical purities of the complexes were more than 95% and the specific activity of all the complexes were > 370 MBq/nmol (radiotracers: excess FA-PEG2-HYNIC > 370 MBq: 1nmol). All of the radiotracers can remain stable in saline and plasma over 6 h.

The log P value of complex **4** in a mixture of phosphate buffer (0.05 mol/L, pH = 7.4) and octanol was -3.40 ± 0.12 , The log P values of complex **5** and **6** were -2.46 ± 0.04 and -3.05 ± 0.35 , respectively.

3.2 *In vitro* cell studies

In vitro cell binding experiments were performed with KB carcinoma cells and mouse normal fibroblast NIH/3T3 cells. KB cells, a human cancer cell line known to highly express FR were used to assess the abilities of ^{99m}Tc -labeled folate conjugates to target the folate receptor.³⁰ NIH/3T3 cells, a mouse normal fibroblast cell line were used as a negative control in this study. As shown in Fig. 4, the complex **4** and **5** displayed a high cell binding properties, $47.60 \pm 8.65\%$ and $50.20 \pm 2.20\%$ of the total

added radioactivity. The internalized fractions of them were $15.12 \pm 3.05\%$ and $16.07 \pm 1.27\%$ of total activity after 1 h incubation. The total binding and the internalized fraction of complex **6** were $34.74 \pm 2.19\%$ and $11.08 \pm 0.73\%$, respectively, which were lower than those of complex **4** and **5** ($p < 0.05$). Pre-incubation of the cells with excess folic acid resulted in almost complete inhibition ($< 1\%$ of the total activity). These data indicate that all the ^{99m}Tc -labeled folate conjugates can target the FR specifically and be internalized in the KB cells. As we expected, all of the complexes displayed less than 0.2% of total added radioactivity of binding in the FR-negative NIH/3T3 cells, which further evidenced the bindings of the ^{99m}Tc -labeled folate conjugates were FR specific.

3.3 Biodistribution studies

The purified radiotracers without cold ligands were used for biodistribution studies. The normal mice biodistribution data of complex **4**, **5** and **6** are shown in Table 1, 2 and 3, respectively. All of the radiolabeled complexes displayed a quick clearance from the blood pool. The renal uptake values of complex **4**, **5** and **6** were $167.85 \pm 6.59\% \text{ID/g}$, $36.07 \pm 9.81\% \text{ID/g}$ and $117.51 \pm 38.9\% \text{ID/g}$ at 1 h post-injection, respectively. The feature of high renal uptake and retention is observed in most folate-based radiotracer as explained before, since the high expression of FR in kidney proximal tubule cells.^{18,29} The blocking study also proved this view, all of the radiotracers displayed a significant reduction of uptake in kidney ($p < 0.05$) after co-injection of excess folic acid ($100\ \mu\text{g}/\text{mouse}$). Among them, the complex **4** exhibited a highest uptake and good retention in FR-positive kidneys, and low uptakes in most organs. Compared to complexes **4** and **6**, complex **5** had lower uptakes in most organs, but showed a significant accumulation of radioactivity in the intestines ($5.09 \pm 1.65\% \text{ID/g}$ at 1h p.i.), suggesting that the radiotracer was excreted quickly via the gastrointestinal tract.

To further investigate the FR binding property of the radiotracer in the tumor model, the tumor uptake and biodistribution properties of complex **4**, **5** and **6** were evaluated in athymic nude mice bearing KB tumors. As shown in Table 4, complex **4** displayed a high tumor uptake ($11.35 \pm 0.67\% \text{ID/g}$ at 2 h

p.i.) and rapid clearance from liver, lungs, blood, muscle and other non-target tissues. At 2 h post-injection, the tumor to liver, tumor to blood and tumor to muscle ratios were 12.80 ± 1.42 , 33.65 ± 11.07 and 13.51 ± 0.65 , respectively. The tumor uptake of complex **6** was 5.52 ± 0.58 %ID/g at 2 h p.i., which was only half of that for complex **4**. At 2 h post-injection, the tumor to liver, tumor to blood and tumor to muscle ratios of complex **6** were 8.89 ± 3.45 , 16.30 ± 5.36 and 4.05 ± 0.61 , respectively. The radioactivity accumulations of complex **6** in intestine and stomach were more than 1 %ID/g at 2 h p.i., which indicated the contribution of gastrointestinal excretion. The complex **5** exhibited a rapid whole-body clearance, and the uptakes in normal organs and tumor (1.24 ± 0.01 %ID/g at 2 h p.i.) were very low except for the kidneys.

In the blocking studies, co-injection of excess folic acid significantly blocked the tumor uptakes of all the radiotracers, as well as the accumulations of radioactivity in the FR-positive kidneys, demonstrating that the tumor and kidney uptakes of the ^{99m}Tc -labeled radiotracers were specific and receptor-mediated.

In order to visualize the distribution of the radiotracer in a living animal, imaging studies of complex **4** were performed in the athymic nude mice bearing KB tumors using a small animal SPECT/CT device. Fig. 5 illustrates the whole-body and transaxial images. Flank KB tumors were clearly visualized at 2 h p.i..

4. Discussion

We have reported a novel class of ^{99m}Tc -HYNIC labeled folate conjugates with a hexane linkers, designed to increase the distance between the targeting moiety and ^{99m}Tc -chelating group previously.¹⁸ Compared with tumor uptake (5.62 ± 0.75 %ID/g at 4 p.i.) of ^{99m}Tc -HYNIC-folate, the tumor uptake of $^{99m}\text{Tc}(\text{HYNIC-NHHN-FA})(\text{tricine/TPPTS})$ increased to $9.79 \pm 1.66\%$ ID/g at 4 h post-injection in the same KB tumor-bearing nude mice.^{18,19} In this study, we used a more hydrophilic and longer linker, PEG2 to replace the hexane linker of $^{99m}\text{Tc}(\text{HYNIC-NHHN-FA})(\text{tricine/TPPTS})$. The distance between the FA targeting moiety and ^{99m}Tc -HYNIC group in $^{99m}\text{Tc}(\text{HYNIC-PEG2-FA})(\text{tricine/TPPTS})$, **4** is two bonds

longer than that of $^{99m}\text{Tc}(\text{HYNIC-NHHN-FA})(\text{tricine/TPPTS})$. The complex **4** ($\log P = -3.40 \pm 0.12$) was more hydrophilic than $^{99m}\text{Tc}(\text{HYNIC-NHHN-FA})(\text{tricine/TPPTS})$ ($\log P = -3.26 \pm 0.08$). The short polyethylene glycol linkers have been used as pharmacokinetic modifying (PKM) linkers to improve the excretion kinetics of radiolabeled small biomolecules, such as bombesin (BBN) peptides³¹⁻³⁴ and α -MSH peptides.^{35,36} For instance, Wang *et al.*³⁴ reported that the polyethylene glycol 4 (PEG4) linkers displayed profound favorable effects on the tumor uptake and pharmacokinetics of radiolabeled cyclic RGD peptides. In this study, PEG2 linker was introduced to improve the excretion kinetics, then to increase target-to-background (T/B) contrast.

Fig. 6 illustrates the comparison of the biodistribution data between complex **4** and $^{99m}\text{Tc}(\text{HYNIC-NHHN-FA})(\text{tricine/TPPTS})$. The data of $^{99m}\text{Tc}(\text{HYNIC-NHHN-FA})(\text{tricine/TPPTS})$ in the same normal mice model were obtained from our previous report. As we anticipated, introduction of a water-soluble linker can enhance the radiotracer excretion from blood, liver, lungs, spleen and other non-target tissues. The blood, liver, lung, spleen uptake of complex **4** were 32% - 65% that of $^{99m}\text{Tc}(\text{HYNIC-NHHN-FA})(\text{tricine/TPPTS})$ at 1 h, 2 h and 4 h after injection, respectively. It is necessary to avoid radioactivity extraction via the gastrointestinal tract, which will interfere with the imaging of abdominal tumor, such as ovarian carcinoma. Compared with $^{99m}\text{Tc}(\text{HYNIC-NHHN-FA})(\text{tricine/TPPTS})$, the radioactivity accumulation in the gastrointestinal tract for complex **4** was significantly decreased. The intestine uptake of complex **4** was only 33% and 12% that of $^{99m}\text{Tc}(\text{HYNIC-NHHN-FA})(\text{tricine/TPPTS})$ at 2 and 4 h after injection, respectively. The tumor uptake of complex **4** was 11.35 ± 0.67 %ID/g at 2 h p.i., which was higher than that of $^{99m}\text{Tc}(\text{HYNIC-NHHN-FA})(\text{tricine/TPPTS})$ (8.92 ± 0.44 %ID/g at 2 h p.i.). The tumor to blood, tumor to liver, tumor to stomach and tumor to intestine ratios of complex **4** were 33.65 ± 11.08 , 12.80 ± 1.42 , 36.94 ± 8.38 and 27.30 ± 9.64 , respectively, which were much better ($p < 0.05$) than those of $^{99m}\text{Tc}(\text{HYNIC-NHHN-FA})(\text{tricine/TPPTS})$ at 2 h p.i. (the ratios were 11.20 ± 3.68 , 8.29 ± 1.12 , 8.63 ± 3.58 and 12.46 ± 0.61 , respectively).¹⁸

We also found that the coligands of ^{99m}Tc -HYNIC labeling moiety had a significant impact on the receptor binding and pharmacokinetic properties of the folate based radiotracers. Although complex **4** and

^{99m}Tc (HYNIC-PEG2-FA)(tricine/TPPMS), **5** had similar FR-specific cell binding and internalized fractions in KB cells *in vitro*, the complex **5** showed low uptake in the FR-positive tissues (1.24 ± 0.01 %ID/g in tumor and 24.38 ± 3.25 %ID/g in kidney at 2 h p.i.) and rapid excretion via the gastrointestinal tract *in vivo*. However, the complex **4** displayed a high uptake and good retention in the FR-positive tissues (11.35 ± 0.67 %ID/g in tumor and 149.70 ± 19.57 %ID/g in kidney at 2 h p.i.). The using of EDDA as coligand to replace the tricine/TPPTS resulted in lower cell binding and internalized fractions in the FR-positive KB cells *in vitro* (Fig. 3). The receptor binding properties difference between ^{99m}Tc (HYNIC-PEG2-FA)(EDDA), **6** and complex **4** is also reflected by their tumor uptakes. The complex **4** has twice the tumor uptake as complex **6** (complex **4**: 11.35 ± 0.67 %ID/g vs complex **6**: 5.52 ± 0.58 %ID/g, $p < 0.05$) in the same animal model with similar tumor size ($0.5 \sim 1.0$ cm³).

For most folate receptor targeted imaging agents, the high liver, gastrointestinal tract and kidney uptakes were the main problems to interfere the tumor imaging. High liver uptake will interfere with the imaging quality of breast and lung tumor, since FR is over-expressed in breast tumor (>60%) and non-small cell lung cancer (>75%).^{15,37,38} The high gastrointestinal tract accumulation as a result of hepatic excretion will interfere with the imaging of abdominal tumor. Hepatic uptake is a common problem in folate radioconjugates. For example, the liver uptake of ^{111}In -DTPA-folate was 9.97 ± 3.28 and 7.32 ± 1.08 %ID/g at 1 h and 4 h p.i. in IGROV-1 tumor-bearing female nude mice.³⁹ At total of 154 patients imaging with ^{99m}Tc -EC20, mild to marked uptake in liver has been seen in all clinical patients.¹⁵ In this study, ^{99m}Tc (HYNIC-PEG2-FA)(tricine/TPPTS), complex **4** has overcome the drawbacks of high liver and gastrointestinal tract uptake of folate radioconjugates. The tumor uptake of complex **4** (11.35 ± 0.67 %ID/g at 2 h p.i.) was comparable to that of ^{99m}Tc -EC20 (11.39 ± 3.24 %ID/g at 1 h p.i. and 12.26 ± 1.05 %ID/g at 4 h p.i.) in the same KB tumor model.⁴⁰ However, the uptakes in liver and intestines of complex **4** (0.89 ± 0.12 %ID/g and 0.27 ± 0.22 %ID/g at 2 h p.i., respectively) were much lower than those of ^{99m}Tc -EC20 (5.12 ± 1.57 %ID/g in liver and 0.95 ± 0.38 %ID/g in intestines at 1 h p.i., 3.06 ± 0.48 %ID/g in liver and 0.51 ± 0.04 %ID/g in intestines at 4 h p.i., respectively).⁴⁰ The tumor to liver

ratio of complex **4** (12.80 ± 1.42 at 2 h p.i.) was approximately four times higher than that of ^{99m}Tc -EC20 (2.28 ± 0.58 at 1 h p.i. and 3.40 ± 1.35 at 4 h p.i.).⁴⁰

However, the complex **4** displayed a high kidney uptake (149.70 ± 19.57 %ID/g in kidney at 2 h p.i.), which is a common disadvantage for most folate receptor targeted imaging agents due to the high expression level of FRs in proximal tubule.^{18,39} The high folate radioconjugates accumulation in kidney leads a high radioactivity dose burden to the kidneys. It also may mask uptake of radioactivity at sites of interest such as small metastases in the abdominal region. Therefore, further reduction of kidney uptake is the biggest challenge for the complex to facilitate clinical evaluation. Three main strategies were undertaken to reduce the kidney uptake: (1) Designation of a folate radioconjugate with albumin-binding entity which can enhance the blood circulation time and then improve the tumor/kidney ratio.^{41,42} It might be an attractive strategy to reduce the kidney uptake of folate radioconjugates, since the kidney retention of ^{177}Lu -cm09 with albumin-binding entity was reduced to 30% of the value of folate conjugate without it.⁴¹ (2) Injection of high dosed amino acids, mainly lysine and arginine, to reduce unspecific accumulation in clinics. But this is not effective for specific binding of folate radioconjugates.^{38,43} (3) Co-injection of succinylated gelatin,⁴³⁻⁴⁵ or combination of folate radioconjugates with antifolates, such as methotrexate, raltitrexed, and pemetrexed, to reduce kidney uptake.⁴⁶ Müller's group found combination of ^{111}In -DTPA-Folate and pemetrexed (PMX) can reduce the kidney uptake and maintain the tumor accumulation.³⁹ PMX is a chemotherapeutic agent which may have toxic side effects. Although, its use for the purpose of improve imaging quality of folate radioconjugates has raised skepticism. Recent study demonstrated that the application of a cocktail containing PMX and thymidine could antagonize the pharmacological and toxic properties of PMX without loss of the desired effect of PMX to reduce the radioactivity accumulation in kidneys.⁴⁶ These findings provide an effective method to improve quality of folate-based nuclear imaging in preclinical research. Therefore, further studies such as the application of PMX or a cocktail containing PMX and thymidine are warranted to prevent the high accumulation in kidneys.

As shown in Fig. 5, the increased tumor uptake and enhanced tumor-to-blood, tumor-to-lung and

tumor-to-gastrointestinal tract ratios of complex **4** generated high contrast between tumor and background in SPECT/CT images. The FR positive KB tumor could be clearly visualized at 2 h p.i. with excellent T/B contrast. Tumor, kidney, bladder were the only visible tissues, the other organs, including liver, gastrointestinal tract, were almost invisible, which was coincident with the trend observed in the biodistribution results, suggesting complex **4** may be worthy of consideration for further pre-clinical development.

5. Conclusion

In this study, a novel folate conjugate FA-PEG2-HYNIC was synthesized and labeled with ^{99m}Tc using tricine/TPPTS, tricine/TPPMS and EDDA as the coligands respectively. It was found that (1) the coligands had a significant effect on the receptor binding and biodistribution properties of the ^{99m}Tc -HYNIC labeled folate-conjugates, (2) PEG2 linker was useful for improving the tumor uptake and clearance kinetics of ^{99m}Tc -labeled folate radiotracers from non-target tissues, especially from liver and gastrointestinal tract, this linker will be a good option for the further designation; (3) ^{99m}Tc (HYNIC-PEG2-FA)(tricine/TPPTS), complex **4** has a good profile with respect to tumor uptake, T/B ratios and pharmacokinetic properties among the ^{99m}Tc -labeled complexes. The FR positive KB tumor could be clearly visualized with high image contrast, highlighting its potential as an effective imaging probe for FR-positive tumor detection.

Acknowledgments

This work was supported by the National Natural Science Foundation of China (20701004, 81201120). The authors would like to thank Prof. Mei Han for her generous help on cell culture.

Notes and references

- 1 H. Elnaka and M. Ratnam, *Adv. Drug Deliv. Rev.*, 2004, **56**, 1067–1084.
- 2 J. F. Ross, P. K. Chaudhuri and M. Ratnam, *Cancer*, 1994, **73**, 2432–2443.

- 3 S. D. Weitman, R. H. Lark, L. R. Coney, D. W. Fort, V. Frasca, V. R. Jr. Zurawski and B. A. Kamen, *Cancer Res.*, 1992, **52**, 3396–3401.
- 4 B. A. Kamen and A. Capdevila, *Proc. Natl. Acad. Sci. U.S.A.*, 1986, **83**, 5983–5987.
- 5 B. Altiparma, F. Y. Lambrecht, E. Bayrak and K. Durkan, *Int. J. Pharm.*, 2010, **400**, 8–14.
- 6 A. R. Hilgenbrink and P. S. Low, *J. Pharm. Sci.*, 2005, **94**, 2135–2146.
- 7 C. P. Leamon and J. A. Reddy, *Adv. Drug Deliv. Rev.*, 2004, **56**, 1127–1141.
- 8 E. I. Segal and P. S. Low, *Cancer Metastasis Rev.*, 2008, **27**, 655–664.
- 9 C. Y. Ke, C. J. Mathias and M. A. Green, *Adv. Drug Deliv. Rev.*, 2004, **56**, 1143–1160.
- 10 C. Müller and R. Schibli, *J. Nucl. Med.*, 2011, **52**, 1–4.
- 11 M. Onursal, F. Y. Lambrecht and A. Ozgur, *Int. J. Pharm.*, 2011, **416**, 288–292.
- 12 C. Y. Ke, C. J. Mathias and M. A. Green, *Nucl. Med. Biol.*, 2003, **30**, 811–817.
- 13 C. J. Mathias, S. Wang, D. J. Waters, J. J. Turek, P. S. Low and M. A. Green, *J. Nucl. Med.*, 1998, **39**, 1579–1585.
- 14 B. A. Siegel, F. Dehdashti, D. G. Mutch, D. A. Podoloff, R. Wendt, G. P. Sutton, R. W. Burt, P. R. Ellis, C. J. Mathias and M. A. Green, *J. Nucl. Med.*, 2003, **44**, 700–707.
- 15 R. E. Fisher, B. A. Siegel, S. L. Edell, N. M. Oyesiku, D. E. Morgenstern, R. A. Messmann and R. J. Amato, *J. Nucl. Med.*, 2008, **49**, 899–906.
- 16 C. P. Leamon, M. A. Parker, I. R. Vlahov, L. C. Xu, J. A. Reddy, M. Vetzal and N. Douglas, *Bioconjug. Chem.*, 2002, **13**, 1200–1210.
- 17 W. Guo, G. H. Hinkle and R. J. Lee, *J. Nucl. Med.*, 1999, **40**, 1563–1569.
- 18 J. Lu, Y. Pang, F. Xie, H. Guo, Y. Li, Z. Yang and X. Wang, *Nucl. Med. Biol.*, 2011, **38**, 557–565.
- 19 L. Q. Liu, S. Z. Wang, F. Li, B. Teng, K. Z. Wang and F. C. Qiu, *Acta. Acad. Med. Sin.*, 2006, **28**, 786–789.
- 20 J. W. Babich and A. J. Fischman, *Nucl. Med. Biol.*, 1995, **22**, 25–30.
- 21 C. Decristoforo and S. J. Mather, *Nucl. Med. Biol.*, 1999, **26**, 389–396.
- 22 S. Liu, W. Y. Hsieh, Y. S. Kim and S. I. Mohammed, *Bioconjug. Chem.*, 2005, **16**, 1580–1588.
- 23 S. Liu, Y. S. Kim, W. Y. Hsieh and S. G. Sreerama, *Nucl. Med. Biol.*, 2008, **35**, 111–121.
- 24 T. D. Harris, M. Sworin, N. Williams, M. Rajopadhye, P. R. Damphousse, D. Glowacka, M. J. Poirier and K.

- Yu, *Bioconjug. Chem.*, 1999, **10**, 808–814.
- 25 R. Schneider, F. Schmitt, C. Frochot, Y. Fort, N. Lourette, F. Guillemin, J. F. Müller and M. Barberi-Heyob, *Bioorg. Med. Chem.*, 2005, **13**, 2799–2808.
- 26 H. Guo, F. Xie, M. Zhu, Y. Li, Z. Yang, X. Wang and J. Lu, *Bioorg. Med. Chem. Lett.*, 2011, **21**, 2025–2029.
- 27 C. Müller, T. L. Mindt, M. De Jong and R. Schibli, *Eur. J. Nucl. Med. Mol. Imaging*, 2009, **36**, 938–946.
- 28 J. Selhub, D. Emmanouel, T. Stavropoulos and R. Arnold, *Am. J. Physiol.*, 1987, **252**, F750–F756.
- 29 H. Birn, S. Nielsen and E. I. Christensen, *Am. J. Physiol.*, 1997, **272**, F70–F78.
- 30 C. Müller, P. A. Schubiger, R. Schibli, *Eur. J. Nucl. Med. Mol. Imaging*, 2006, **33**, 1162–1170.
- 31 J. C. Garrison, T. L. Rold, G. L. Sieckman, F. Naz, S. V. Sublett, S. D. Figueroa, W. A. Volert and T. J. Hoffman, *Bioconjug. Chem.*, 2008, **19**, 1803–1812.
- 32 S. Liu, Z. He, W. Y. Hsieh, Y. S. Kim and Y. Jiang, *Bioconjug. Chem.*, 2006, **17**, 1499–1507.
- 33 J. Shi, L. Wang, Y. S. Kim, S. Zhai, Z. Liu, X. Chen and S. Liu, *J. Med. Chem.*, 2008, **51**, 7980–7990.
- 34 L. Wang, J. Shi, Y. S. Kim, S. Zhai, B. Jia, H. Zhao, Z. Liu, F. Wang, X. Chen and S. Liu, *Mol. Pharm.*, 2008, **6**, 231–245.
- 35 H. Guo, J. Yang, F. Gallazzi and Y. Miao, *J. Nucl. Med.*, 2011, **52**, 608–616.
- 36 Y. Miao, F. Gallazzi, H. Guo and T. P. Quinn, *Bioconjug. Chem.*, 2008, **19**, 539–547.
- 37 C. Gridelli and M. D. Maio, *Expert Opin. Pharmacother.*, 2010, **11**, 321–324.
- 38 C. Müller and R. Schibli, *Front Oncol.*, 2013, **3**, 249
- 39 C. Müller, R. Schibli, E. P. Krenning and M. De Jong, *J. Nucl. Med.*, 2008, **49**, 623–629.
- 40 C. Müller, J. A. Reddy, C. P. Leamon and R. Schibli, *Mol. Pharm.*, 2010, **7**, 597–604.
- 41 C. R. Fischer, V. Groehn, J. Reber, R. Schibli, S. M. Ametamey and C. Müller, *Mol. Imaging Biol.*, 2013, **15**, 649–654.
- 42 C. Müller, H. Struthers, C. Winiger, K. Zhernoseko and R. Schibli, *J. Nucl. Med.*, 2013, **54**, 124–131.
- 43 E. J. Rolleman, M. Melis, R. Valkema, O. C. Boerman, E. P. Krenning and M. De Jong, *Eur. J. Nucl. Med. Mol. Imaging*, 2010, **37**, 1018–1031.
- 44 E. Vegt, J. F. Wetzels, G. M. Russel, R. Masereeuw, O. C. Boerman, J. E. van Eerd, H. M. Corstens and J. G. Oyen, *J. Nucl. Med.*, 2006, **47**, 432–436.

45 A. Briat, H. F. Wenk, M. Ahnadi, M. Claron, D. Boturyn, V. Josserand, P. Dumy, D. Fagret, J. Coll, C.

Ghezzi, L. Sancey and J. Vuillez, *Cancer Sci.*, 2012, **103**, 1105–1110.

46 C. Müller, J. Reber, C. Schlup, C. P. Leamon and R. Schibli, *Mol. Pharm.*, 2013, **10**, 967–974.

Figure captions

Fig. 1. The structures of NHHN-FA, PEG2-FA and ^{99m}Tc -HYNIC labeled folate conjugates with different co-ligands.

Fig. 2. The synthesis of conjugate HYNIC-PEG2-FA. *i.* DCC, DMSO/pyridine, RT, 18 h; *ii.* TFA, 0 °C, 2 h; *iii.* NHS-HYNIC, DMSO/pyridine, RT, 18 h.

Fig. 3. HPLC profiles of radioactive of ^{99m}Tc labeled HYNIC-PEG2-FA. The retention time of $^{99m}\text{Tc}(\text{HYNIC-PEG2-FA})(\text{tricine})$ (**A**), $^{99m}\text{Tc}(\text{HYNIC-PEG2-FA})(\text{tricine/TPPTS})$, **4** (**B**), $^{99m}\text{Tc}(\text{HYNIC-PEG2-FA})(\text{tricine/TPPMS})$, **5** (**C**) and $^{99m}\text{Tc}(\text{HYNIC-PEG2-FA})(\text{EDDA})$, **6** (**D**) were 15.4 min, 22.5 min, 28.3 min and 21.4 min, respectively.

Fig. 4. *In vitro* experiment of the all the complexes with KB cells; cell total binding, internalization and blocked by excess folic acid ($p < 0.05$). The cell bindings were calculated per 0.5 mg protein and expressed as percentage of total added radioactivity.

Fig. 5. Whole-body (A) and transaxial images (B) of complex **4** in the athymic nude mice bearing KB tumors (female, 18~20 g) at 120 min p.i. Arrows indicate the presence of tumors.

Fig. 6. The comparison of the biodistribution data between complex **4** and $^{99m}\text{Tc}(\text{HYNIC-NHHN-FA})(\text{tricine/TPPTS})$ in the normal mice fed with a folate-free diet for 7 days before the experiments.

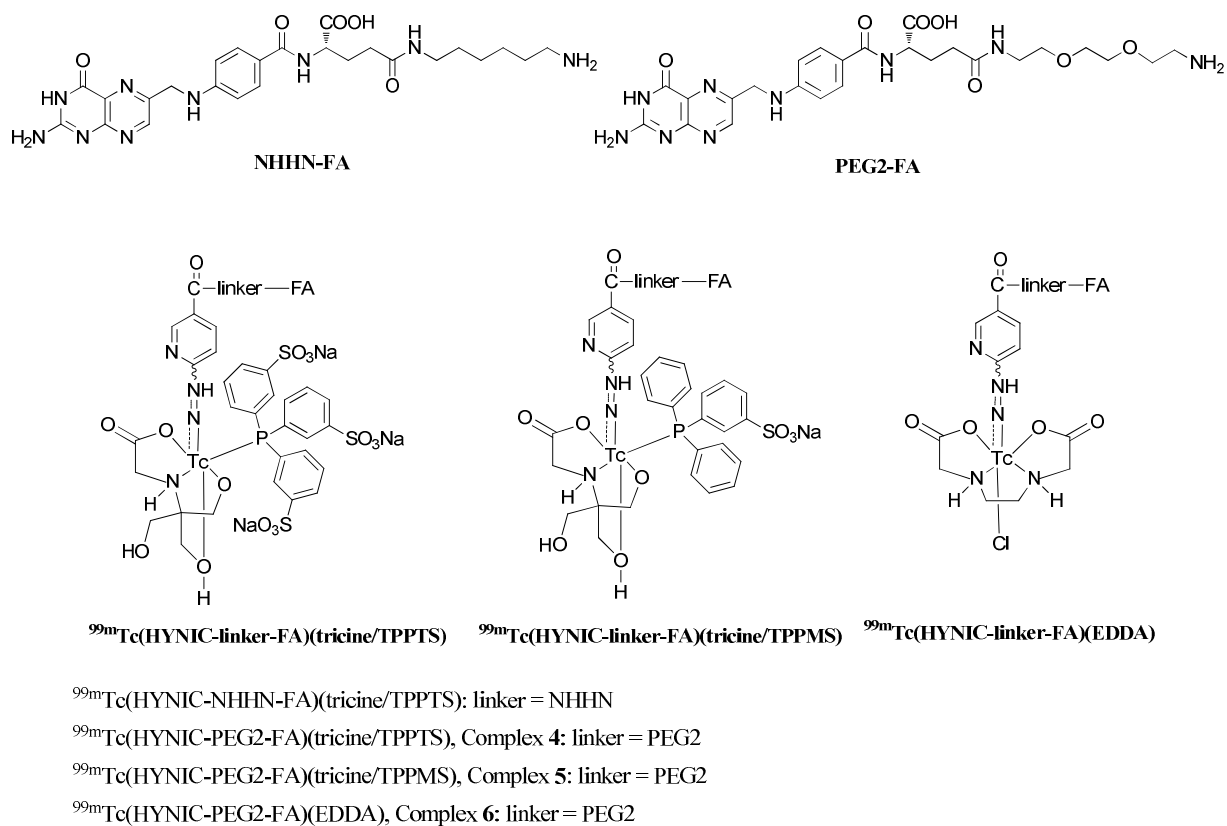


Fig. 1. The structures of NHHN-FA, PEG2-FA and ^{99m}Tc -HYNIC labeled folate conjugates with different co-ligands.

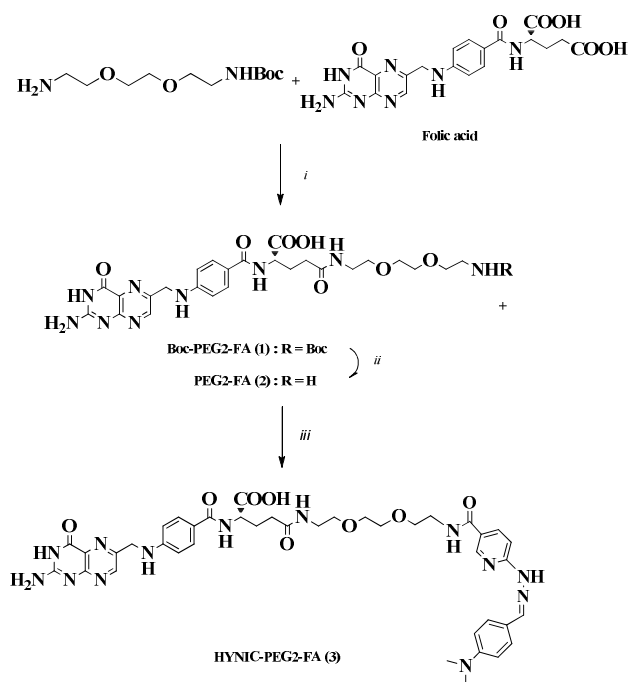


Fig. 2. The synthesis of conjugate HYNIC-PEG2-FA. *i.* DCC, DMSO/pyridine, RT, 18 h; *ii.* TFA, 0 °C, 2 h; *iii.* NHS-HYNIC, DMSO/pyridine, RT, 18 h.

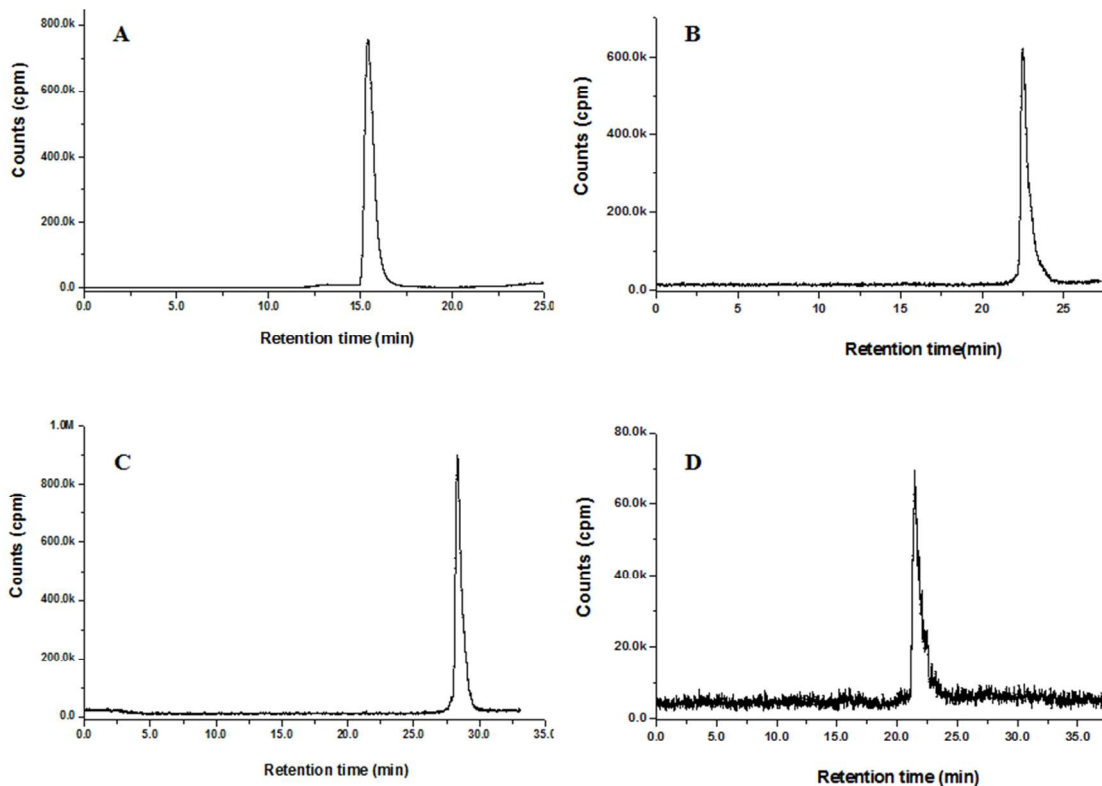


Fig. 3. HPLC profiles of radioactive of ^{99m}Tc labeled HYNIC-PEG2-FA. The retention time of $^{99m}\text{Tc}(\text{HYNIC-PEG2-FA})(\text{tricine})$ (**A**), $^{99m}\text{Tc}(\text{HYNIC-PEG2-FA})(\text{tricine}/\text{TPPTS})$, **4** (**B**), $^{99m}\text{Tc}(\text{HYNIC-PEG2-FA})(\text{tricine}/\text{TPPMS})$, **5** (**C**) and $^{99m}\text{Tc}(\text{HYNIC-PEG2-FA})(\text{EDDA})$, **6** (**D**) were 15.4 min, 22.5 min, 28.3 min and 21.4 min, respectively.

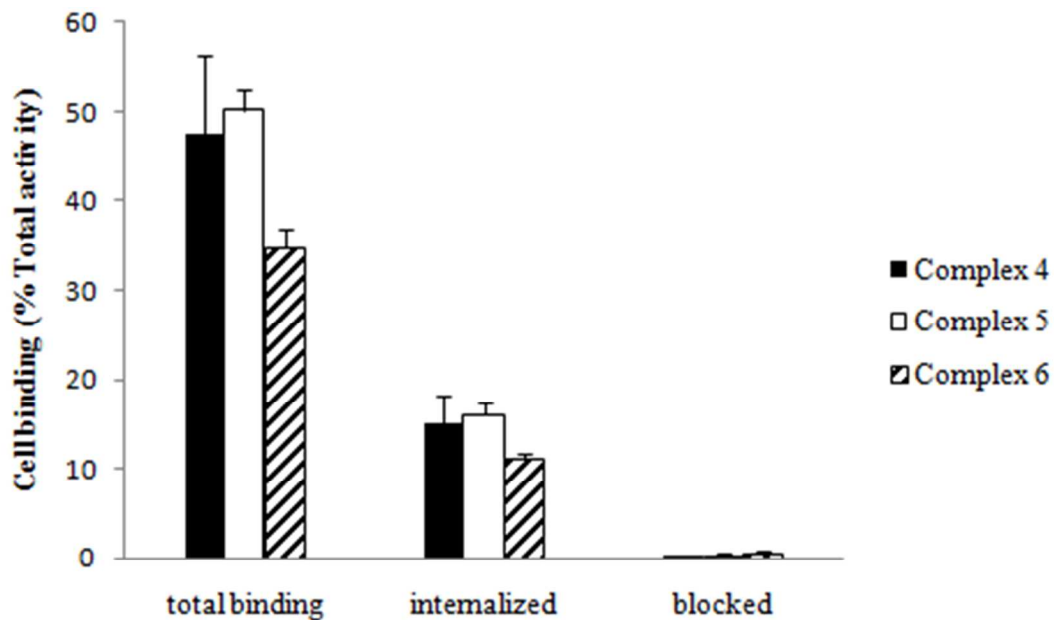


Fig. 4. *In vitro* experiment of the all the complexes with KB cells; cell total binding, internalization and blocked by excess folic acid ($p < 0.05$). The cell bindings were calculated per 0.5 mg protein and expressed as percentage of total added radioactivity.

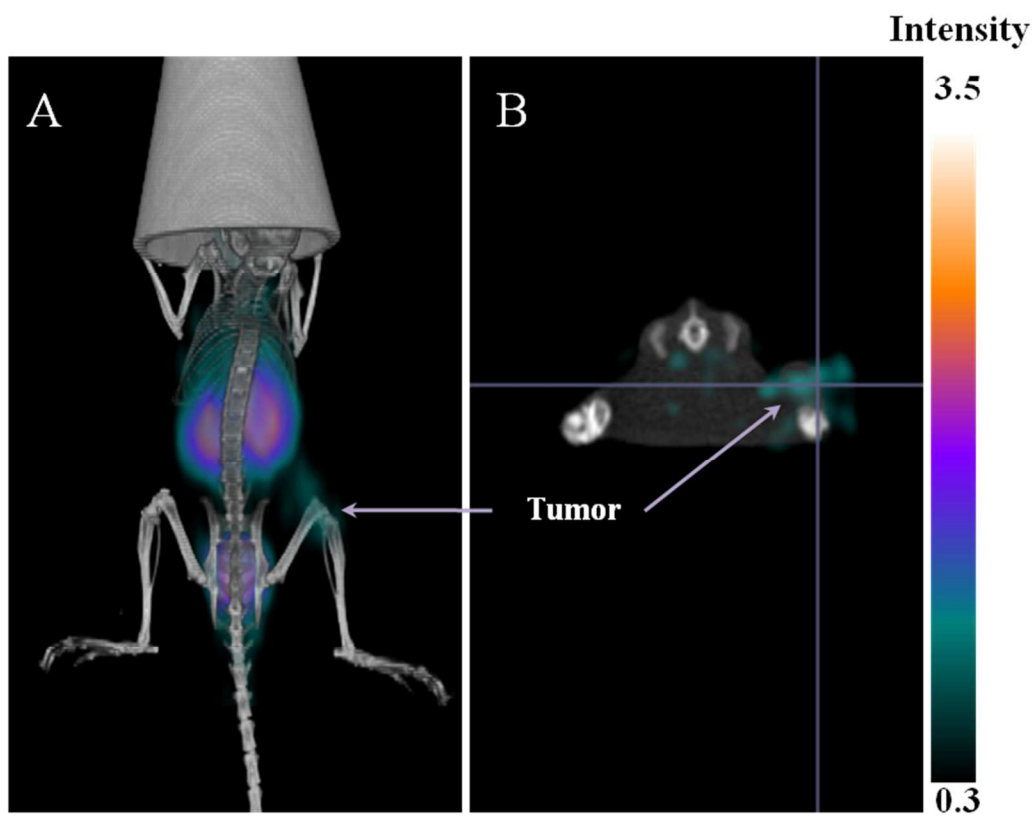


Fig. 5. Whole-body (A) and transaxial images (B) of complex 4 in the athymic nude mice bearing KB tumors (female, 18~20 g) at 120 min p.i. Arrows indicate the presence of tumors.

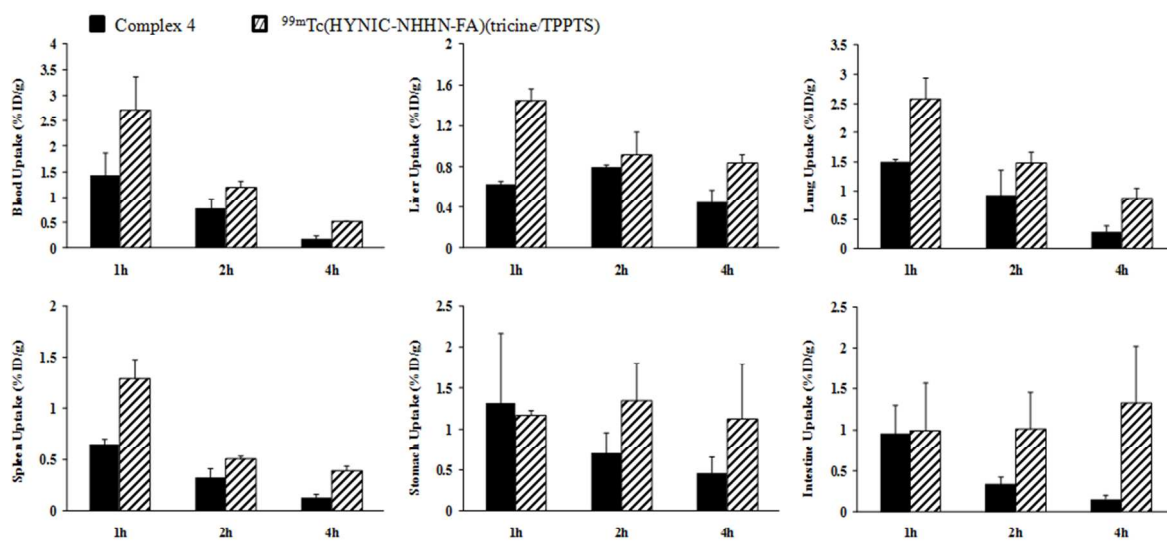


Fig. 6. The comparison of the biodistribution data between complex 4 and $^{99m}\text{Tc}(\text{HYNIC-NHHN-FA})(\text{tricine/TPPTS})$ in the normal mice fed with a folate-free diet for 7 days before the experiments.

Table 1. Biodistribution of $^{99m}\text{Tc}(\text{HYNIC-PEG2-FA})(\text{tricine/TPPTS})$, **4** in normal mice

Tissue	1h	1h- blockade	2h	4h
Heart	1.19 ± 0.46	0.21 ± 0.10	0.59 ± 0.13	0.28 ± 0.01
Liver	0.63 ± 0.04	0.37 ± 0.07	0.80 ± 0.03	0.45 ± 0.13
Lungs	1.49 ± 0.06	0.81 ± 0.51	0.91 ± 0.44	0.28 ± 0.12
Spleen	0.66 ± 0.05	0.19 ± 0.07	0.33 ± 0.09	0.13 ± 0.04
Kidney	167.85 ± 6.59	5.65 ± 1.53*	132.66 ± 7.21	93.29 ± 2.55
Bone	0.43 ± 0.20	0.40 ± 0.03	0.19 ± 0.09	0.08 ± 0.02
Intestine and contents	0.96 ± 0.35	0.28 ± 0.15	0.34 ± 0.09	0.16 ± 0.05
Muscle	0.93 ± 0.25	0.15 ± 0.06	0.53 ± 0.20	0.16 ± 0.05
Stomach	1.32 ± 0.85	1.34 ± 0.61	0.71 ± 0.25	0.47 ± 0.20
Blood	1.44 ± 0.45	0.47 ± 0.21	0.79 ± 0.19	0.17 ± 0.08

Data are expressed as %ID/g (mean ± S.D., n = 5)

* $p < 0.05$, significance comparison on kidney uptakes between complex **4** with or without folate blockade at 1 h post-injection.

Table 2. Biodistribution of $^{99m}\text{Tc}(\text{HYNIC-PEG2-FA})(\text{tricine}/\text{TPPMS})$, **5** in normal mice

Tissue	1h	1h-blockade	2h	4h
Heart	0.25 ± 0.08	0.21 ± 0.07	0.18 ± 0.08	0.09 ± 0.07
Liver	0.55 ± 0.19	1.17 ± 0.36	0.27 ± 0.07	0.22 ± 0.08
Lungs	0.52 ± 0.09	0.40 ± 0.06	0.25 ± 0.08	0.17 ± 0.06
Spleen	0.18 ± 0.08	0.20 ± 0.06	0.12 ± 0.04	0.10 ± 0.04
Kidney	36.07 ± 9.81	1.51 ± 0.22*	33.21 ± 9.82	20.21 ± 9.16
Bone	0.17 ± 0.03	0.19 ± 0.10	0.19 ± 0.02	0.14 ± 0.06
Intestine and contents	5.09 ± 1.65	3.64 ± 2.61	1.91 ± 0.49	3.29 ± 2.58
Muscle	0.26 ± 0.07	0.16 ± 0.05	0.26 ± 0.10	0.08 ± 0.04
Stomach	0.33 ± 0.08	0.16 ± 0.07	0.45 ± 0.19	0.72 ± 0.29
Blood	0.26 ± 0.10	0.18 ± 0.01	0.11 ± 0.03	0.08 ± 0.03

Data are expressed as %ID/g (mean ± S.D., n = 5)

* $p < 0.05$, significance comparison on kidney uptakes between complex **5** with or without folate blockade at 1 h post-injection.

Table 3. Biodistribution of $^{99m}\text{Tc}(\text{HYNIC-PEG2-FA})(\text{EDDA})$, **6** in normal mice

Tissue	1h	1h-blockade	2h	4h
Heart	0.65 ± 0.13	0.44 ± 0.18	0.62 ± 0.34	0.28 ± 0.04
Liver	0.69 ± 0.11	0.52 ± 0.07	0.69 ± 0.18	0.46 ± 0.04
Lungs	0.99 ± 0.16	0.75 ± 0.21	0.56 ± 0.20	0.21 ± 0.16
Spleen	0.65 ± 0.24	0.47 ± 0.17	0.42 ± 0.32	0.10 ± 0.11
Kidney	117.51 ± 38.9	3.67 ± 0.78*	105.56 ± 11.55	90.76 ± 39.42
Bone	0.68 ± 0.12	0.54 ± 0.20	0.33 ± 0.09	0.18 ± 0.13
Intestine and contents	1.04 ± 0.53	0.66 ± 0.16	0.89 ± 0.86	0.71 ± 0.18
Muscle	0.48 ± 0.11	0.31 ± 0.13	0.51 ± 0.21	0.10 ± 0.11
Stomach	2.96 ± 0.56	1.89 ± 0.59	2.39 ± 0.42	0.52 ± 0.83
Blood	0.87 ± 0.14	0.65 ± 0.17	0.39 ± 0.11	0.16 ± 0.02

Data are expressed as %ID/g (mean ± S.D., n = 5)

* $p < 0.05$, significance comparison on kidney uptakes between complex **6** with or without folate blockade at 1 h post-injection.

Table 4. Biodistribution of the radiotracers in KB tumor-bearing mice

	Complex 4		Complex 5		Complex 6	
	2 h	2 h-blockade	2 h	2h-blockade	2 h	2h-blockade
<i>Tissue</i>						
Heart	1.06 ± 0.28	0.28 ± 0.19	0.17 ± 0.04	0.14 ± 0.02	1.33 ± 0.10	0.75 ± 0.17
Liver	0.89 ± 0.12	0.65 ± 0.27	0.90 ± 0.03	1.00 ± 0.30	1.36 ± 0.32	0.33 ± 0.05
Lungs	0.79 ± 0.35	0.76 ± 0.34	2.27 ± 0.90	2.22 ± 0.30	1.05 ± 0.24	0.54 ± 0.20
Spleen	0.47 ± 0.47	0.24 ± 0.12	0.69 ± 0.35	0.41 ± 0.06	0.66 ± 0.23	0.42 ± 0.14
Kidney	149.70 ± 19.57	24.56 ± 9.27*	24.38 ± 3.25	1.76 ± 0.61*	121.41 ± 11.5	3.26 ± 0.96*
Intestine and contents	0.27 ± 0.22	0.21 ± 0.15	0.35 ± 0.12	0.37 ± 0.22	1.40 ± 1.13	1.34 ± 0.64
Stomach	0.68 ± 0.36	0.16 ± 0.08	1.56 ± 1.03	1.13 ± 1.07	1.70 ± 0.36	1.01 ± 0.24
Blood	0.37 ± 0.13	0.49 ± 0.17	0.15 ± 0.06	0.10 ± 0.00	0.11 ± 0.02	0.28 ± 0.17
Muscle	0.85 ± 0.12	0.30 ± 0.08	0.15 ± 0.02	0.16 ± 0.03	0.73 ± 0.36	0.92 ± 0.43
Tumor	11.35 ± 0.67	0.65 ± 0.28*	1.24 ± 0.01	0.21 ± 0.08*	5.52 ± 0.58	0.48 ± 0.15*
<i>Ratios</i>						
Tumor/Blood	33.65 ± 11.07	-	8.29 ± 0.91	-	16.30 ± 5.36	-
Tumor/Muscle	13.51 ± 0.65	-	8.87 ± 1.49	-	8.89 ± 3.41	-
Tumor/Liver	12.80 ± 1.42	-	1.32 ± 0.17	-	4.05 ± 0.61	-

Date are expressed as %ID/g (mean ± S.D., n = 3)

* $p < 0.05$, significance comparison on tumor and kidney uptakes between the radiotracers with or without folate blockade at 2 h post-injection.

Graphical abstract

The novel complex $^{99m}\text{Tc}(\text{FA-PEG2-HYNIC})(\text{tricine}/\text{TPPTS})$ was clearly visualized at 120 min p.i. at the FR-positive tumor, highlighting its potential as an effective folate receptor tumor imaging agent.

